Letter

Signatures of quantum chaos and fermionization in the incoherent transport of bosonic carriers in the Bose-Hubbard chain

P. S. Muraev,[1,2,3] D. N. Maksimov,[1,3] and A. R. Kolovsky[1,2]

[1]*Kirensky Institute of Physics, Federal Research Centre KSC SB RAS, 660036 Krasnoyarsk, Russia*

[2]*School of Engineering Physics and Radio Electronics, Siberian Federal University, 660041 Krasnoyarsk, Russia*

[3]*IRC SQC, Siberian Federal University, 660041 Krasnoyarsk, Russia*

(Received 29 July 2023; accepted 27 February 2024; published 22 March 2024)

We analyze the stationary current of Bose particles across the Bose-Hubbard chain connected to a battery, focusing on the effect of interparticle interactions. It is shown that the current magnitude drastically decreases as the strength of interparticle interactions exceeds the critical value which marks the transition to quantum chaos in the Bose-Hubbard Hamiltonian. We found that this transition is well reflected in the nonequilibrium many-body density matrix of the system. Namely, the level-spacing distribution for eigenvalues of the density matrix changes from Poisson to Wigner-Dyson distributions. With the further increase of the interaction strength, the Wigner-Dyson spectrum statistics change back to the Poisson statistics which now marks fermionization of the Bose particles. With respect to the stationary current, this leads to the counter-intuitive dependence of the current magnitude on the particle number.

DOI: 10.1103/PhysRevE.109.L032107

Recently, we have seen a surge of interest to quantum transport in one-dimensional systems coupled at their edges to particle reservoirs [1–22]. Following [1] we refer to these systems as boundary driven systems. Particularly, one very important example of the boundary driven system is the so-called open Bose-Hubbard (BH) model or BH chain [7–16]. This system can be realized experimentally by using different physical platforms including superconducting circuits [17,18], photonic crystals [19,20], and cold Bose atoms in optical lattices [21]. The central question to be addressed with the open BH chain, both theoretically and experimentally, is the stationary current of Bose particles across the chain and its dependence on the strength of interparticle interactions. It is known that properties of the closed/conservative BH system crucially depend on the ratio of the hopping matrix element J and the interaction constant U which are two of the four parameters of the BH Hamiltonian, the other being the chain length L and the particle number N. For example, for integer N/L the ground state of the system shows the quantum phase transition between the super-fluid state for $J \gg U$ and the Mott-insulator state in the opposite limit [23]. As for the excited states they show a qualitative change from the regular to the chaotic [24,25]. Thus, one may expect that the stationary current in the open BH chain should also crucially depend on the interaction constant.

To approach the formulated problem we introduce a specific boundary driven BH model which conserves the number of particles in the system. Although the introduced model cannot be directly related to ongoing laboratory experiments, it admits a comparative theoretical analysis with the closed BH system. In this paper we compare the energy spectrum of the closed system with the eigenspectrum of the stationary density matrix of the open system. It is found that the spectrum of the stationary density matrix shows the same structural changes as the energy spectrum of the BH Hamiltonian when the control parameter (in our case, the interaction constant U) is varied. We also demonstrate that the observed changes in the spectrum statistics are well reflected in the stationary current across the BH chain which, unlike the spectrum statistic, is a measurable quantity. Last but not least, the introduced model allows for the exact numerical analysis of relative large systems which is unfeasible in the case of the common boundary driven BH model. For example, for the common model with $L = 10$ and the mean number of particle $\langle N\rangle = 5$, one has to account for particle number fluctuations at least until $N_{\max} = 10$. This gives the density matrix of the size larger than $150\,000 \times 150\,000$, as compared to the matrix size 2002×2002 in the case of the fixed $N = 5$.

We consider the BH chain of the length L with incoherent coupling between the first and the $L_{\rm th}$ sites. The coupling is described by the the following Lindblad operators:

$$\mathcal{L}_1(\widehat{R}) = \widehat{V}^\dagger\widehat{V}\widehat{R} + \widehat{R}\widehat{V}^\dagger\widehat{V} - 2\widehat{V}\widehat{R}\widehat{V}^\dagger,$$
$$\mathcal{L}_2(\widehat{R}) = \widehat{V}\widehat{V}^\dagger\widehat{R} + \widehat{R}\widehat{V}\widehat{V}^\dagger - 2\widehat{V}^\dagger\widehat{R}\widehat{V}, \qquad (1)$$

where $\widehat{V} = \hat{a}_1^\dagger\hat{a}_L$ [22,26,27]. Thus, the master equation for the carrier density matrix $\widehat{R}$ reads

$$\frac{\partial\widehat{R}}{\partial t} = -i[\widehat{H},\widehat{R}] - \Gamma_1\mathcal{L}_1(\widehat{R}) - \Gamma_2\mathcal{L}_2(\widehat{R}), \qquad (2)$$

where

$$\widehat{H} = -\frac{J}{2}\sum_{\ell=1}^{L-1}(\hat{a}_{\ell+1}^\dagger\hat{a}_\ell + \text{H.c.}) + \frac{U}{2}\sum_{\ell=1}^{L}\hat{n}_\ell(\hat{n}_\ell - 1) \qquad (3)$$

is the Bose-Hubbard Hamiltonian. It is easy to see that the Lindblad operator $\mathcal{L}_1(\widehat{R})$ induces the incoherent transport of

 ©2024 American Physical Society

the carriers from the last to the first sites, while the operator $\mathcal{L}_2(\widehat{R})$ is responsible for the incoherent transport in the reverse direction. If the rates $\Gamma_1 \neq \Gamma_2$, there is a nonzero current in the clockwise or counterclockwise direction depending on the inequality relationship between the two relaxation constants. We notice that, by an analogy with electronic devices, the introduced Lindblad operators mimic the effect of a battery which induces direct current in the electric circuits.

We are interested in the stationary current $I = \mathrm{Tr}[\widehat{I}\widehat{R}]$ where $\widehat{R} = \widehat{R}(t \to \infty)$ is now the steady-state density matrix and $\widehat{I}$ is the current operator,

$$\widehat{I} = \frac{J}{2i}\sum_{\ell=1}^{L-1}(\hat{a}^{\dagger}_{\ell+1}\hat{a}_{\ell} - \mathrm{H.c.}). \tag{4}$$

First of all, we notice that if $\Gamma_1 = \Gamma_2$ the steady-state density matrix is proportional to the identity matrix, namely, $\widehat{R} = \widehat{1}/\mathcal{N}$, where $\mathcal{N}$ is the dimension of the Hilbert space. In what follows we focus on the liner response regime where $\Gamma_1 = \Gamma + \Delta\Gamma/2$, $\Gamma_2 = \Gamma - \Delta\Gamma/2$, and $\Delta\Gamma \ll \Gamma$. Thus, we have

$$\widehat{R} = \frac{\widehat{1}}{\mathcal{N}} + \Delta\Gamma\widetilde{R}, \tag{5}$$

where $\mathrm{Tr}[\widetilde{R}] = 0$. Substituting the Ansatz (5) into the master equation, we obtain

$$-i[\widehat{H}, \widetilde{R}] - \Gamma[\mathcal{L}_1(\widetilde{R}) + \mathcal{L}_2(\widetilde{R})] - \frac{2(\hat{n}_L - \hat{n}_1)}{\mathcal{N}} = O(\Delta\Gamma). \tag{6}$$

In the limit $\Delta\Gamma \to 0$, Eq. (6) transforms into the algebraic equation for the elements of the unknown matrix $\widetilde{R}$. In our numerical approach, however, we do not solve this algebraic equation but evolve the density matrix $\widehat{R}(t)$ according to the master equation (2) and use Eq. (6) to check that we reached the true steady state. We found this method to be more efficient than the straightforward solution of the algebraic equation.

Since our primary goal is the stationary current across the chain, we shall analyze the matrix $\widetilde{R}$ in the basis of the eigenstates of the current operator,

$$\widehat{I} = \sum_{j=1}^{\mathcal{N}} \sigma_j |\Phi_j\rangle\langle\Phi_j|. \tag{7}$$

Two examples of the matrix $\widetilde{R}$ in this basis are given in Fig. 1 for $U = 0$, left panel, and $U = J$, right panel. A qualitative difference between these two cases is clearly visible from the plot. In the next paragraph we quantify this difference. We conclude the present paragraph by displaying the commutation relation between the current operator and the BH Hamiltonian for $U = 0$,

$$-i[\widehat{H}, \widehat{I}] - \frac{(\hat{n}_L - \hat{n}_1)}{2} = 0, \tag{8}$$

which we shall use later on.

Knowing that the BH Hamiltonian (3) exhibits transition to quantum chaos as U is increased, we expect a similar transition for the nonequilibrium density matrix. This expectation is supported by the visual analysis of the matrices depicted in Fig. 1 and results of the relevant studies of the boundary driven

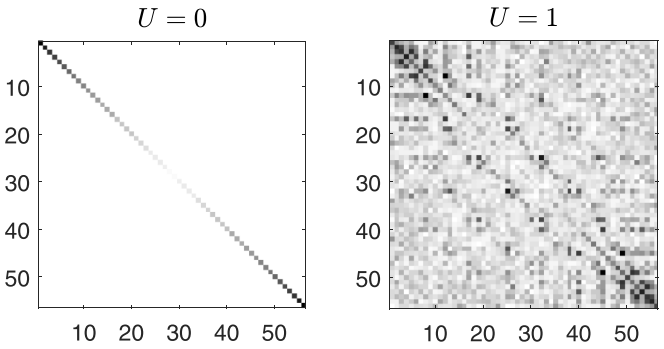

FIG. 1. Absolute values of the matrix elements of the matrix $\widetilde{R}$ in the basis of the current operator. The system parameters are $L = 6$, $N = 3$ (the Hilbert space dimension $\mathcal{N} = 56$), $J = 1$, $\Gamma = 0.04$, and $U = 0$ (left) and $U = 1$ (right). The upper limit of the color axis is 0.2.

spin chains [28,29]. Following Refs. [28,29], we consider the spectrum and eigenstates of the nonequilibrium density matrix,

$$\widetilde{R} = \sum_{j=1}^{\mathcal{N}} \lambda_j |\Psi_j\rangle\langle\Psi_j|. \tag{9}$$

In what follows we restrict ourselves by the case $\Gamma \ll J$. Then, if $U = 0$, the states $|\Psi_j\rangle$ practically coincide with the eigenstates of the current operator $|\Phi_j\rangle$, while the eigenvalues are related to each other as

$$\lambda_j \approx 4\sigma_j/\mathcal{N}. \tag{10}$$

To see that, let us scale the density matrix $\widetilde{R} \to \mathcal{N}/4 \cdot \widetilde{R}$ and set $\Delta\Gamma = 0$ in Eq. (6). Then the obtained algebraic equation differs from the commutation relation Eq. (8) by a small term $\sim\Gamma$ which can be taken into account perturbatively. As expected, application of the perturbation theory removes degeneracies of the eigenvalues of the current operator, see the inset (b) in Fig. 2.

The magenta staircase curve in Fig. 2 depicts the case $U \neq 0$. Here we see that the width of the spectrum increases as U is increased. The main difference is, however, in the spectrum statistics. Figure 3 shows the distribution of the the scaled spacings $s = (\lambda_{j+1} - \lambda_j)f(\lambda_j)$, with $f(\lambda)$ being the mean density of states, as compared to the Poisson and Wigner-Dyson distributions [30]. For $U = J$ a nice agreement with the Wigner-Dyson distribution, which is the hallmark of quantum chaos [31,32], is noticed.

Next we analyze the stationary current I across the chain:

$$I = \mathrm{Tr}[\widehat{I}\widehat{R}] = \sum_{j=1}^{\mathcal{N}} \lambda_j \langle\Psi_j|\widehat{I}|\Psi_j\rangle \equiv \sum_{j=1}^{\mathcal{N}} \lambda_j I_j. \tag{11}$$

In the case of vanishing interparticle interactions, one derives by using Eq. (10) the following semianalytic equation:

$$I = 4JN^2\Delta\Gamma \int_0^1 \sigma^2(x)dx, \tag{12}$$

where $x = j/\mathcal{N}$ and $\sigma(x)$ is the inverse function to the integrated density of states of the current operator, which interpolates the blue line in Fig. 2. Thus, as it is intuitively

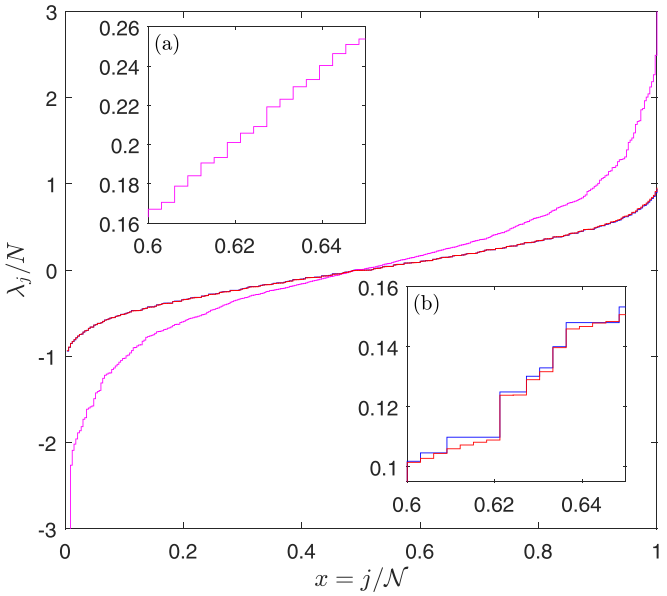

FIG. 2. The scaled eigenvalues of the matrix $\widetilde{R}$ for $U = 0$, red line, and $U = 1$, magenta line, compared to the eigenvalues of the current operator, blue line. Parameters are $L = 8$, $N = 4$ ($\mathcal{N} = 330$), $J = 1$, and $\Gamma = 0.04$.

expected, for $U = 0$ the total current increases with the number of particles in the system.

The case $U \neq 0$ is more subtle. Figure 4 shows numerically obtained dependence of the stationary current on the interaction constant U for $L = 6$ and a different number of particles N. One clearly identifies in Fig. 4(b) the critical $U_{cr} = U_{cr}(\bar{n})$, $\bar{n} = N/L$, above which the current drastically decreases. This critical interaction marks the crossover from the Poisson to the Wigner-Dyson spectrum statistics for the nonequilibrium density matrix $\widetilde{R}$. An unexpected result is that for $U \gg U_{cr}$ the current decreases with the number of particles. Furthermore, we find that for these large U the spectrum statistics is again Poissonian.

We relate the observed change of the spectrum statistics and the counterintuitive dependence of the current on the particle number to the interaction-induced localization of the eigenstates $|\Psi_j\rangle$ and the fermionization of the strongly interacting Bose particles [33]. Indeed, the obvious consequence of the eigenstate localization is that the mean $I_j = \langle\Psi_j|\widehat{I}|\Psi_j\rangle$ tends to zero and is strictly zero if all bosons occupies a single site of the chain. Figure 5 shows the quantiles I_j for $(L, N) = (6, 3)$ and $U = 0, 0.5, 10$. It is seen that the fraction of the delocalized states which support the current decreases in favor of the localized states for which $I_j \approx 0$. For example, in Fig. 5(c) the states corresponding to the minimal and maximal eigenvalues are the states $|\Psi_1\rangle \approx |0, 0, 0, 0, 0, 3\rangle$ and $|\Psi_{\mathcal{N}}\rangle \approx |3, 0, 0, 0, 0, 0\rangle$. Along with the localized and partially localized states, one can see in Fig. 5(c) a number of the delocalized states. A closer inspection of these states shows that they are a superposition of the Fock states where occupation numbers of the chain sites are either zero or unity. Since this subspace of the Hilbert space is the Hilbert space of the hard-core bosons, we conclude that the residual conductivity of the system at large U is mainly due to the

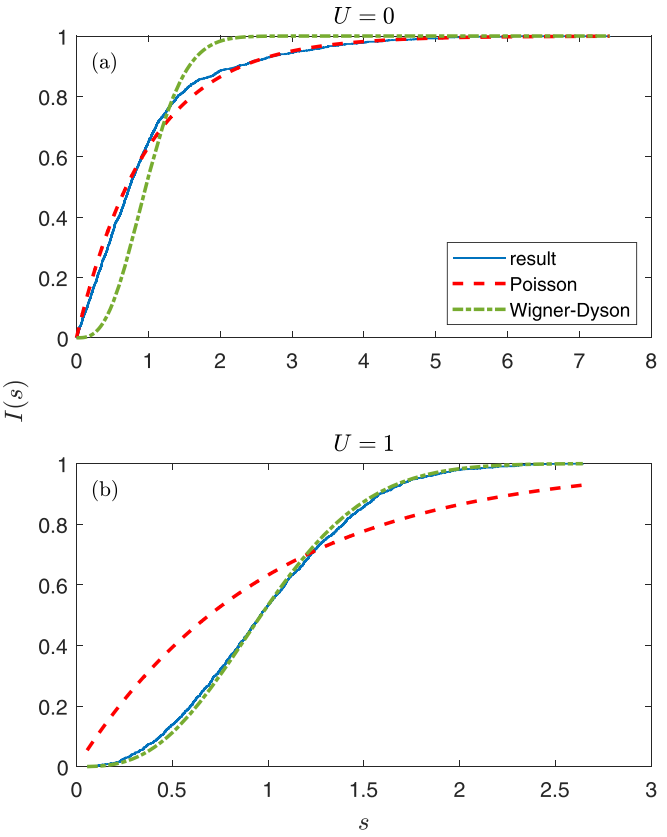

FIG. 3. The integrated level spacing distribution compared to the integrated Poisson and GUE Wigner-Dyson distributions for $U = 0$ (a) and for $U = 1$ (b). The other parameters are $L = 10, N = 5$ ($\mathcal{N} = 2002$), and $\Gamma = 0.04$. For the statistical analysis we took 60 percent of eigenvalues from the central part of the spectrum.

hard-core bosons. As is known, the spectral and transport properties of the hard-core bosons are similar to those of the noninteracting fermions and, hence, they can support ballistic

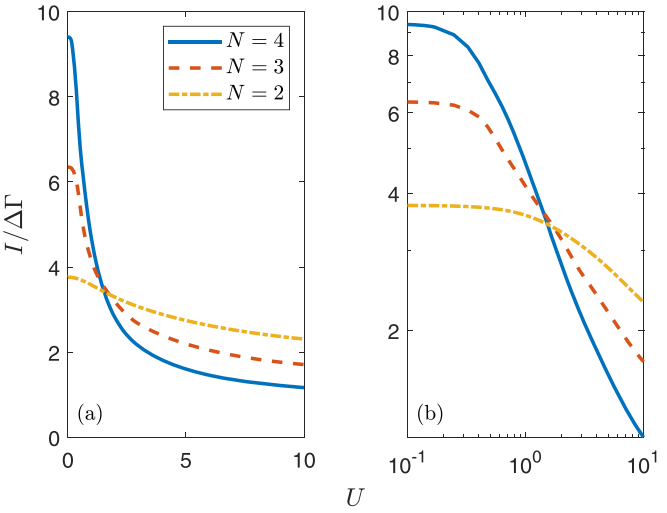

FIG. 4. The total current as a function of the interaction constant U for three different values of the particle number $N = 2, 3, 4$ in the linear (a) and logarithmic (b) scales, $L = 6$ and $\Gamma = 0.04$.

transport for arbitrary large U if $N/L < 1$. We also mention that the appearance of the localized states and the integrable states associated with the hard-core bosons is consistent with the observed change of the level-spacing distribution from the Wigner-Dyson distribution back to the Poisson distribution in the limit of large U.

In summary, we introduced the model for quantum transport of Bose particles across the Bose-Hubbard chain which conserves the number of particles in the chain. Similar to the standard transport model where a Bose-Hubbard chain connects two particle reservoirs with different chemical potentials and where the number of particles is not conserved, the introduced model shows different transport regimes depending on the ratio between the tunneling and interaction constants in the Bose-Hubbard Hamiltonian (3). Namely, for $U \sim J$ the stationary current of the Bose particles is drastically suppressed as compared to the case $U = 0$. In our previous publication [9] we explain this effect by transition to chaotic dynamics of the classical counterpart of the system. In this work we use the genuine quantum approach where the object of interest is the nonequilibrium many-body density matrix of the bosonic carriers in the chain. This is a unique example where the nonequilibrium density matrix is calculated/analyzed for the nonintegrable bosonic system. (For transport properties of the fermionic and spin systems we refer the reader to the recent review [34]). We found the spectrum of this matrix exhibits a transition from a regular spectrum for $U \ll J$, which obeys the Poisson statistics, to an irregular spectrum for $U \sim J$, which obeys the Wigner-Dyson statistics. In this sense we confirm the conjecture of Ref. [9] that the drastic reduction of the current for $U \sim J$ is due to the transition to quantum chaos.

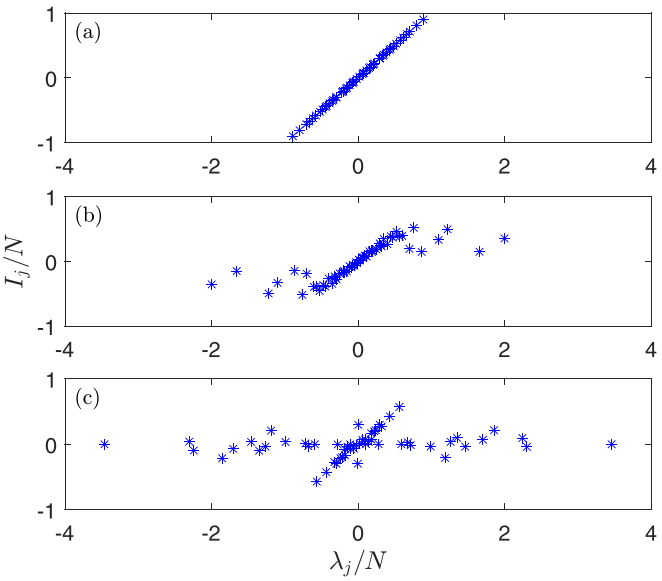

FIG. 5. The quantities $I_j = \langle \Psi_j | \widehat{I} | \Psi_j \rangle$ for $U = 0$ (a), 0.5 (b), and 10 (c). The system parameters are $L = 6$, $N = 3$, and $\Gamma = 0.04$.

Within the framework of the introduced model we also observed an interesting effect—the residual conductivity due to fermionization of Bose particles. We notice that this is a pure quantum effect which cannot be addressed by using the classical (mean-field) or pseudoclassical (truncated Wigner function) approaches.

The authors acknowledge financial support from the Ministry of Science and Higher Education of Russian Federation (Project No. FSRZ-2023-0006).

[1] G. T. Landi, D. Poletti, and G. Schaller, Nonequilibrium boundary-driven quantum systems: Models, methods, and properties, Rev. Mod. Phys. **94**, 045006 (2022).

[2] D. Manzano, M. Tiersch, A. Asadian, and H. J. Briegel, Quantum transport efficiency and Fourier's law, Phys. Rev. E **86**, 061118 (2012).

[3] S. Ajisaka, F. Barra, C. Mejía-Monasterio, and T. Prosen, Nonequlibrium particle and energy currents in quantum chains connected to mesoscopic Fermi reservoirs, Phys. Rev. B **86**, 125111 (2012).

[4] T. Jin, M. Filippone, and T. Giamarchi, Generic transport formula for a system driven by Markovian reservoirs, Phys. Rev. B **102**, 205131 (2020).

[5] A.-M. Visuri, T. Giamarchi, and C. Kollath, Symmetry-protected transport through a lattice with a local particle loss, Phys. Rev. Lett. **129**, 056802 (2022).

[6] S. Uchino, Comparative study for two-terminal transport through a lossy one-dimensional quantum wire, Phys. Rev. A **106**, 053320 (2022).

[7] A. Ivanov, G. Kordas, A. Komnik, and S. Wimberger, Bosonic transport through a chain of quantum dots, Eur. Phys. J. B **86**, 345 (2013).

[8] A. R. Kolovsky, Z. Denis, and S. Wimberger, Landauer-Büttiker equation for bosonic carriers, Phys. Rev. A **98**, 043623 (2018).

[9] A. A. Bychek, P. S. Muraev, D. N. Maksimov, and A. R. Kolovsky, Open Bose-Hubbard chain: Pseudoclassical approach, Phys. Rev. E **101**, 012208 (2020).

[10] P. S. Muraev, D. N. Maksimov, and A. R. Kolovsky, Resonant transport of bosonic carriers through a quantum device, Phys. Rev. A **105**, 013307 (2022).

[11] G. Kordas, D. Witthaut, P. Buonsante, A. Vezzani, R. Burioni, A. I. Karanikas, and S. Wimberger, The dissipative Bose-Hubbard model, Eur. Phys. J.: Spec. Top. **224**, 2127 (2015).

[12] G. Kordas, D. Witthaut, and S. Wimberger, Non-equilibrium dynamics in dissipative Bose-Hubbard chains, Ann. Phys. **527**, 619 (2015).

[13] P. Manasi and D. Roy, Light propagation through one-dimensional interacting open quantum systems, Phys. Rev. A **98**, 023802 (2018).

[14] T. Haug, H. Heimonen, R. Dumke, L.-C. Kwek, and L. Amico, Aharonov-Bohm effect in mesoscopic Bose-Einstein condensates, Phys. Rev. A **100**, 041601 (2019).

[15] C. Lledó and M. H. Szymańska, A dissipative time crystal with or without $\mathbb{Z}_2$ symmetry breaking, New J. Phys. **22**, 075002 (2020).

[16] F. Ferrari, L. Gravina, D. Eeltink, P. Scarlino, V. Savona, and F. Minganti, Steady-state quantum chaos in open quantum systems, arXiv:2305.15479.

[17] M. Fitzpatrick, N. M. Sundaresan, A. C. Y. Li, J. Koch, and A. A. Houck, Observation of a dissipative phase transition in a one-dimensional circuit QED lattice, Phys. Rev. X **7**, 011016 (2017).

[18] G. P. Fedorov, S. V. Remizov, D. S. Shapiro, W. V. Pogosov, E. Egorova, I. Tsitsilin, M. Andronik, A. A. Dobronosova, I. A. Rodionov, O. V. Astafiev, and A. V. Ustinov, Photon transport in a Bose-Hubbard chain of superconducting artificial atoms, Phys. Rev. Lett. **126**, 180503 (2021).

[19] A. Szameit, D. Blömer, J. Burghoff, T. Schreiber, T. Pertsch, S. Nolte, A. Tünnermann, and F. Lederer, Discrete nonlinear localization in femtosecond laser written waveguides in fused silica, Opt. Express **13**, 10552 (2005).

[20] G. Cáceres-Aravena, D. Guzmán-Silva, I. Salinas, and R. A. Vicencio, Controlled transport based on multiorbital Aharonov-Bohm photonic caging, Phys. Rev. Lett. **128**, 256602 (2022).

[21] R. Labouvie, B. Santra, S. Heun, and H. Ott, Bistability in a driven-dissipative superfluid, Phys. Rev. Lett. **116**, 235302 (2016).

[22] L. Garbe, Y. Minoguchi, J. Huber, and P. Rabl, The bosonic skin effect: Boundary condensation in asymmetric transport, SciPost Phys. **16**, 029 (2024).

[23] M. Greiner, O. Mandel, T. Esslinger, T. W. Hänsch, and I. Bloch, Quantum phase transition from a superfluid to a Mott insulator in a gas of ultracold atoms, Nature (London) **415**, 39 (2002).

[24] A. R. Kolovsky and A. Buchleitner, Quantum chaos in the Bose-Hubbard model, Europhys. Lett. **68**, 632 (2004).

[25] A. R. Kolovsky, Bose–Hubbard Hamiltonian: Quantum chaos approach, Int. J. Mod. Phys. B **30**, 1630009 (2016).

[26] T. Haga, M. Nakagawa, R. Hamazaki, and M. Ueda, Liouvillian skin effect: Slowing down of relaxation processes without gap closing, Phys. Rev. Lett. **127**, 070402 (2021).

[27] Y. Minoguchi, J. Huber, L. Garbe, A. Gambassi, and P. Rabl, A unified interface model for dissipative transport of bosons and fermions, arXiv:2311.10138.

[28] T. Prosen and M. Žnidarič, Eigenvalue statistics as an indicator of integrability of nonequilibrium density operators, Phys. Rev. Lett. **111**, 124101 (2013).

[29] M. Žnidarič, Magnetization transport in spin ladders and next-nearest-neighbor chains, Phys. Rev. B **88**, 205135 (2013).

[30] E. P. Wigner, On the statistical distribution of the widths and spacings of nuclear resonance levels, Math. Proc. Camb. Philos. Soc. **47**, 790 (1951).

[31] F. Haake, Quantum signatures of chaos, in *Quantum Coherence in Mesoscopic Systems*, edited by B. Kramer (Springer US, Boston, MA, 1991), pp. 583–595.

[32] H.-J. Stöckmann, *Quantum Chaos: An Introduction* (Cambridge University Press, Cambridge, 1999).

[33] B. Paredes, A. Widera, V. Murg, O. Mandel, S. Fölling, I. Cirac, G. V. Shlyapnikov, T. W. Hänsch, and I. Bloch, Tonks–Girardeau gas of ultracold atoms in an optical lattice, Nature (London) **429**, 277 (2004).

[34] B. Bertini, F. Heidrich-Meisner, C. Karrasch, T. Prosen, R. Steinigeweg, and M. Žnidarič, Finite-temperature transport in one-dimensional quantum lattice models, Rev. Mod. Phys. **93**, 025003 (2021).